Is the longitudinal distribution of H_2O ice different on Miranda compared to the other Uranian satellites?

David DeColibus[1], Nancy Chanover[1], Richard Cartwright[2]
([1]New Mexico State University, [2]SETI Institute)

Background

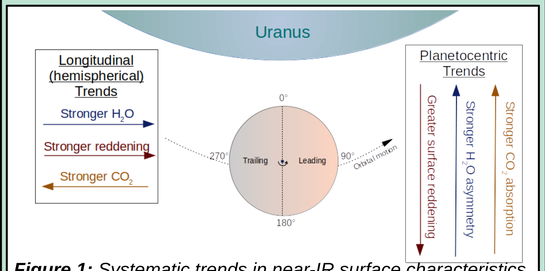

Figure 1: *Systematic trends in near-IR surface characteristics on the four large Uranian satellites.*

- In the Uranian system [1-4], the leading (apex) hemispheres of the classical satellites show stronger near-IR H_2O ice absorption features compared to the trailing (antapex) hemispheres (**Fig. 1**). This leading/trailing asymmetry is stronger closer to Uranus and decreases with increasing planetocentric distance.
- This pattern is an expected result of exogenic processes, including impacts and irradiation by the co-rotating magnetosphere of the host planet [4-6].
- Previous observations of the innermost moon Miranda suggest that it does not show a similar leading/trailing asymmetry in H_2O ice, although the processes that should produce that asymmetry should operate most strongly on Miranda [4]. Miranda does not show evidence of either CO_2 ice or a longitudinal reddening pattern [4].
- Imaging of Miranda's southern hemisphere during the *Voyager* 2 flyby in 1986 (**Fig. 2**) revealed bizarre geological features [7], with ancient, cratered plains contrasted with young (≤1 Gyr, [8]) regions of heavily tectonically modified ridges and troughs.

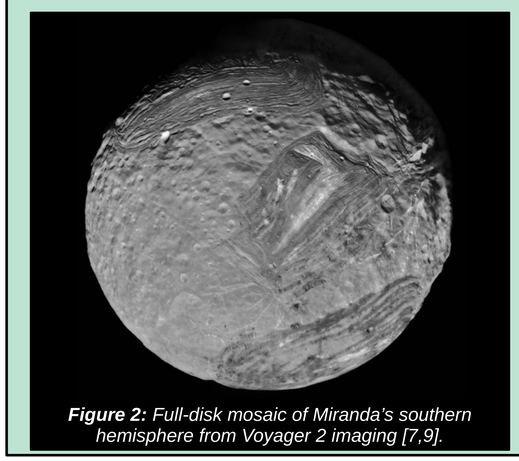

Figure 2: *Full-disk mosaic of Miranda's southern hemisphere from Voyager 2 imaging [7,9].*

Observations

- We acquired 22 new NIR spectra of Miranda's northern hemisphere with the ARC 3.5m/TripleSpec spectrograph and 2 new spectra with Gemini North/GNIRS (**Fig. 3**).
- We also included 7 published and 3 previously unpublished NIR spectra from the IRTF/SpeX spectrograph [4,10].
- This combined dataset represents a substantial improvement in the NIR spectroscopic longitudinal coverage of Miranda (**Fig. 4**).

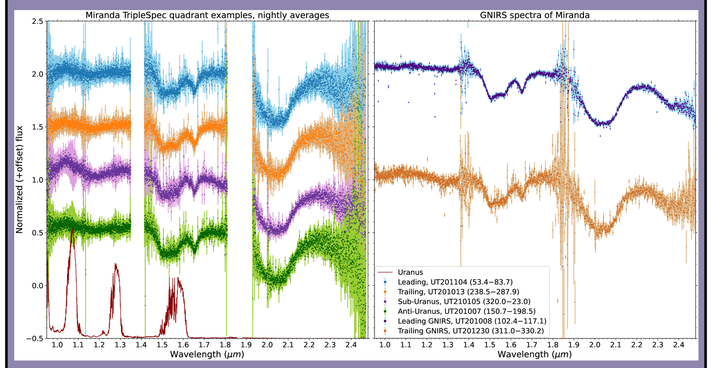

Figure 3: *Examples of our TripleSpec nightly-average spectra (left panel) and our two GNIRS spectra (right panel). Scattered light from Uranus was corrected by subtracting a scaled spectrum of Uranus from each Miranda spectrum.*

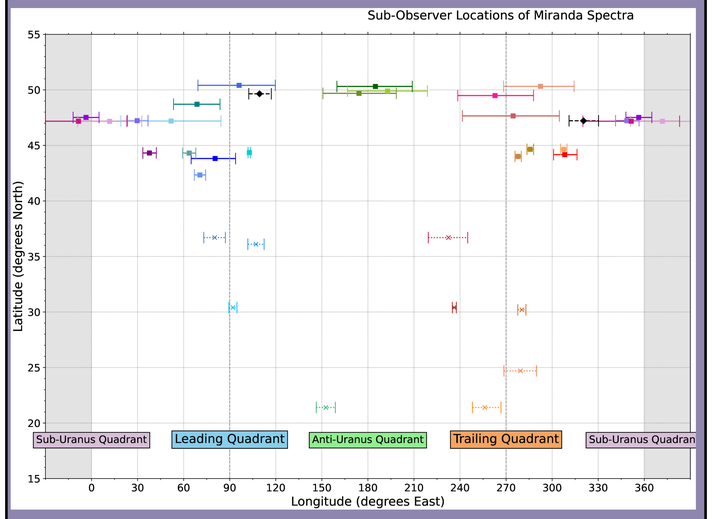

Figure 4. *A latitude-longitude plot of our spectral coverage, where horizontal errorbars illustrate the range of sub-Earth longitudes during acquisition of each spectrum. Spectra at latitudes >35°N are new in this work. Squares are TripleSpec data, Xs are SpeX data, and black diamonds are GNIRS data.*

Methods

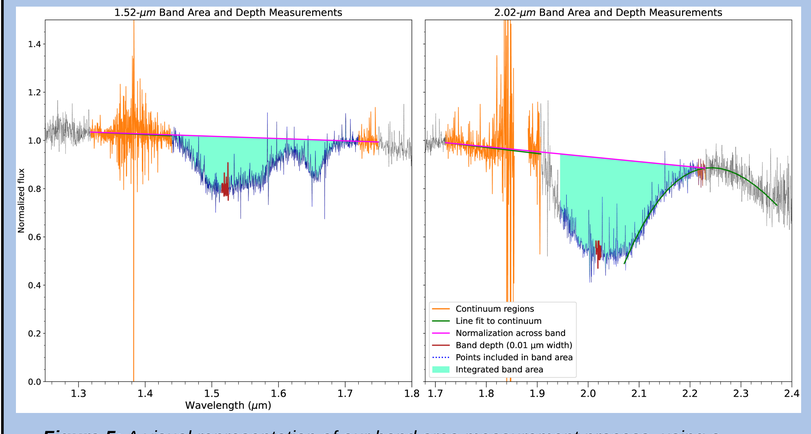

Figure 5: *A visual representation of our band area measurement process, using a TripleSpec spectrum of Miranda gathered on UT 2021/01/01.*

- For each of our spectra, we measured the integrated band areas and fractional band depths of the 1.5-μm and 2.0-μm H_2O ice bands (**Fig. 5**), using a custom code based on the methodology used in [3,4].
- To measure the integrated band areas, we draw a continuum line between two defined regions on either side of the absorption band, normalize the spectrum by this line, then integrate the area inside the absorption band.
- The same normalization line is used to measure the fractional band depth, taking the mean relative reflectance of the points ±0.005 μm of the defined centers of the absorption bands (1.52 and 2.02 μm).

Results

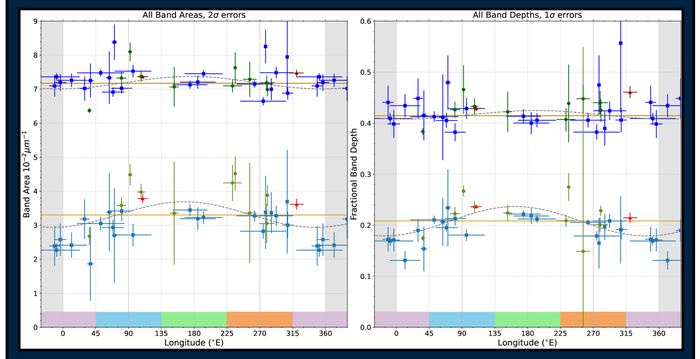

Figure 6: *The variation of band areas (left panel) and depths (right panel) with longitude on Miranda's northern hemisphere. The upper set of measurements is the 2.0-μm band, and the lower set is the 1.5-μm band. Blue squares are TripleSpec spectra, green circles are SpeX spectra, and red triangles are GNIRS spectra. The best-fit constant and sinusoidal models are solid yellow lines and gray dashed lines, respectively.*

- A sinusoidal model provides a statistically significant better fit than a constant model to the variation of band areas and depths with longitude for the 1.5-μm H_2O ice band, but not for the 2.0-μm H_2O ice band (**Table 1**).
- However, instead of the expected leading/trailing asymmetry, the sinusoidal model fits an asymmetry between the sub-Uranus and anti-Uranus regions of Miranda's surface (**Fig. 6**).
- We also calculated ratios of mean band strength between opposing quadrants of Miranda's surface (**Table 2**).
- There is a statistically significant asymmetry in the 1.5-μm band areas and depths between the anti-Uranus and sub-Uranus quadrants, but effectively no asymmetry between the leading and trailing quadrants or hemispheres.
- There is no statistically significant asymmetry in the 2.0-μm H_2O ice band, regardless of which opposing quadrants or hemispheres are considered.

Dataset	Measurement	N	Longitude max absorption (°)	F-value	*p*-value	Reject null hypothesis?
All spectra	1.52-μm area	34	166.4	4.569	0.01824	Yes
	1.52-μm depth	34	162.9	13.404	0.00006	Yes
	2.02-μm area	34	174.6	1.596	0.21892	No
	2.02-μm depth	34	191.4	0.834	0.44380	No

Table 1: *We present the results of our F-test analysis. N refers to the number of data points (spectra) included in our model fits. We reject the null hypothesis if the p-value calculated from the F-test is p ≤0.05.*

Dataset	Ratio[a]	1.52-μm band		2.02-μm band	
		Area ratio	Depth ratio	Area ratio	Depth ratio
All spectra	LQ/TQ	0.98 ± 0.08	1.10 ± 0.21	1.03 ± 0.03	0.99 ± 0.06
	LH/TH	0.97 ± 0.07	1.04 ± 0.14	1.00 ± 0.02	0.99 ± 0.04
	AQ/SQ	1.26 ± 0.13	1.27 ± 0.09	1.01 ± 0.02	0.97 ± 0.04
Miranda	LH/TH	0.94 ± 0.18	···	0.95 ± 0.09	···
Ariel	LH/TH	1.46 ± 0.06	···	1.27 ± 0.03	···
Umbriel	LH/TH	1.21 ± 0.096	···	1.14 ± 0.038	···
Titania	LH/TH	1.15 ± 0.033	···	1.11 ± 0.034	···
Oberon	LH/TH	1.09 ± 0.0465	···	1.09 ± 0.023	···

Table 2: *We present ratios between the mean band measurements for opposing quadrants and hemispheres of Miranda's surface. L, T, A, and S refer to leading, trailing, anti-Uranus, and sub-Uranus, respectively, while Q indicates the average is over a quadrant, and H refers to average over a hemisphere. All errors are 1σ errors. At the bottom of the table we include the leading/trailing hemisphere ratios for Miranda and the other Uranian satellites reported in Cartwright et al. (2018).*

Conclusions

- **There is no statistically-significant asymmetry between the leading and trailing hemispheres of Miranda in the strength of the near-IR H_2O ice absorption bands.**
- The depth of absorption features in H_2O ice is not solely controlled by abundance. Other effects like grain size [5,6] and low-albedo contaminants [11] can play a substantial role.
- More exotic explanations may be at play, such as complex magnetospheric irradiation effects, polar reorientation of Miranda [12], a lack of spectral 'masking' by CO_2 ice [13], mantling by icy or dusty ring particles [4,14], or the effects of geological activity, such as resurfacing or plume deposits [14].
- **The apparent anti-Uranus/sub-Uranus asymmetry in the strength of the 1.5-μm band also suggests that there is more to Miranda's H_2O ice than an explanation based on a simple leading/trailing model would account for.**
- Our upcoming paper and our future work will investigate our findings in more detail.

Could Miranda be an ocean world?

- Previous authors have noted the parallels between Miranda and the similarly-sized, active ocean world Enceladus [e.g. 14,15], including the positioning of tectonically-modified regions on their surfaces attributed to internal upwelling [16] (**Fig. 2**).
- A previous detection of an absorption feature at 2.2 μm on Miranda has been attributed to NH_3-hydrate [17], and a similar absorption band was recently confirmed on Ariel and may be due to NH_3/NH_4-bearing species [18]. The exact identity of the absorber(s) is an open question.
- NH_3 is a potent antifreeze and is thought to enable endogenic activity and possibly the retention of internal oceans on icy satellites [e.g. 19].
- Our future work with our dataset will explore the implications of our results in more detail and put constraints on the presence of volatile species on Miranda's surface, but **only a Uranus orbiter mission could answer this question definitively [20].**

References and Acknowledgements

[1] Grundy et al. (2003), *Icarus*, 162, 222.
[2] Grundy et al. (2006), *Icarus*, 184, 543.
[3] Cartwright et al. (2015), *Icarus*, 257, 428.
[4] Cartwright et al. (2018), *Icarus*, 314, 210.
[5] Clark et al. (1983), *Icarus*, 56, 233.
[6] Clark et al. (1984), *Icarus*, 58, 265.
[7] Smith et al. (1986), *Science*, 233, 43.
[8] Zahnle et al. (2003), *Icarus*, 163, 263.
[9] Stryk & Stooke (2008), *LPSC*, 39, 1362.
[10] Gourgeot et al. (2014), *A&A*, 562, A46.
[11] Clark & Lucey (1984), *JGR*, 89, 6341.
[12] Pappalardo & Greeley (1993), *LPSC*, 24, 1111.
[13] Cartwright et al. (2020a), *Icarus*, 338, 113513.
[14] Cartwright et al. (2020b), *LPSC*, 51, 1699.
[15] Pappalardo & Schubert (2013), *LPSC*, 44, 2808.
[16] Pappalardo et al. (1997), *JGR*, 102, 13369.
[17] Bauer et al. (2002), *Icarus*, 158, 178.
[18] Cartwright et al. (2020c), *ApJL*, 898, L22.
[19] Kargel (1992), *Icarus*, 100, 556.
[20] Cartwright et al. (2021), *PSJ*, 2, 120.

This research was funded under NASA FINESST grant award number NSSC20K1378. This work makes use of new observations acquired with the Astrophysical Research Consortium 3.5m telescope at Apache Point Observatory, new observations acquired under program ID GN-2020B-FT-205 at the Gemini North telescope, and observations previously obtained at the Infrared Telescope Facility (IRTF), which is operated by the University of Hawaii under contract 80HQTR19D0030 with the National Aeronautics and Space Administration. We extend our appreciation and thanks to the support staff at these facilities that made this project possible.